# Fabrication of Porous Polyimide Membrane with Through-Hole via Multiple Solvent Displacement Method

Sho Hirai,*[a] Patchiya Phanthong,*[a] Tsubasa Wakabayashi,[b] and Shigeru Yao[a, b]

Porous polyimide (PI) membranes are widely used in separation processes because of their excellent thermal and mechanical properties. However, the applications of porous PI membranes are limited in the nanofiltration range. In this study, porous PI membranes with through-holes have been successfully fabricated by the novel multiple solvent displacement method. This new method requires only a porous polyamic acid (PAA) membrane, which was prepared by immersing PAA film in N-methylpyrrolidoneebk; (NMP) prior to immersing it in a mixed solvent consisting of NMP and a poor solvent, followed by immersion only in poor solvent. The pore size, morphology, porosity, and air permeability demonstrated that the fabricated PI membranes had a uniformly porous structure with through-holes over their surface. This new method enabled control of pore size (3–11 μm) by selecting a suitable poor solvent. This multiple solvent displacement method is highly versatile and promising for the fabrication of porous PI membranes.

## 1. Introduction

Porous membranes are one of the most commonly used forms in separation for various fields. They are not only applied in the industry, but also in general households. Examples of porous membrane applications include the separation of oil and gas,[1] lithium-ion batteries,[2] biological cells,[3] and waste water treatment.[4] Porous membranes can be divided into various types based on their separation capabilities, such as microfiltration (MF), ultrafiltration (UF), nanofiltration (NF), and reverse osmosis (RO).[5] Due to the fact that the demand for porous membranes is expected to increase in near future,[6] an environmentally friendly fabrication process for high performance of separation is attractive.[7] Generally, top-down and bottom-up approaches are used to fabricate a porous membrane. Top-down approaches include lithography or similar methods, which can be fabricated the porous membranes with a microstructure.[8] Bottom-up approaches involve the self-organization of porous polymer structures.[9] However, both approaches have some defects, for example the limitation of applicable polymers and difficulties for scaling up to desirable manufacturing volumes.

Owing to the multifunctionality and ease of fabrication, polymeric porous membranes have gained much more attraction in research.[10] The common types of polymer used in the fabrication of polymeric porous membranes include polyethylene,[11] polystyrene,[12] polyethylene terephthalate,[13] and poly(ether sulfone).[14] The selection of the polymer type is dependent on the solvent and the feed, which are the targets for separation.

Polymeric porous membranes have been fabricated based on a phase separation mechanism. Thermally induced phase separation (TIPS) is one of the common fabricating method.[15] TIPS can induce phase separation in polymer solutions by cooling them from a high-temperature state. This homogeneous porous membrane has been successfully fabricated with various sizes by simply controlling the combination of the solvent and the different cooling rates.[16,17] However, TIPS has some drawbacks, especially when slight differences in the cooling rate or type of solvent significantly affect to the pore size of the fabricated porous membrane. For this reason, innovative methods for controlling the pore size are desired. Another method that easily enables phase separation in a polymer solution is non-solvent-induced phase separation (NIPS).[18] NIPS is a method of fabricating a porous membrane by immersing a polymer solution in a poor solvent using the principle of phase separation. In NIPS, rapid phase separation can occur at the contact surface between the polymer solution and the non-solvent. From this reason, the dense thin layer is performed at that contact interface. With the covering by the dense thin layer, the micron-sized porous membrane fabricated from NIPS method is not suitable.

Polyimide (PI) is a polymeric material which feature high heat stability, insulation properties, and mechanical strength.[19,20] With these outstanding properties, PI has been widely used in various applications such as motor vehicles, electronic materials, and pharmaceutical products. Recently, PI has been considered to fabricate porous membranes owing to its high affinity for various substances, easy polymerization, and high potential for functionalization by chemical modification or combination with other organic and inorganic materials.[21]

[a] Dr. S. Hirai, Dr. P. Phanthong, Prof. S. Yao
Research Institute for the Creation of Functional and Structural Materials
Fukuoka University
8-19-1 Nanakuma, Jonan-ku, Fukuoka 814-0180 (Japan)
E-mail: shohirai@fukuoka-u.ac.jp
patchiya@fukuoka-u.ac.jp
[b] T. Wakabayashi, Prof. S. Yao
Graduate School of Chemical Engineering
Fukuoka University
8-19-1 Nanakuma, Jonan-ku, Fukuoka 814-0180 (Japan)

Presently, porous PI membranes are fabricated via the NIPS method; hence, most PI membranes can only be used for nanofiltration (NF) applications such as gas separation.[22] Nevertheless, expanding the applicability of the porous PI membrane to the microfiltration (MF) range is highly attractive. With its excellent thermal stability, chemical resistance, and high mechanical strength, porous PI membranes in the MF range are preferred over existing MF membranes. Several approaches have been developed to control the pore size of porous PI membranes and thereby expand their applicability from the NF to MF range or various other fields.[23] Kim et al. fabricated a porous PI membrane with a pore size of 0.1–10 μm by controlling the height of the solvent according to Jurin's Law.[24] However, the development of facile fabricating methods to produce a homogeneous micron-sized porous membrane has still remains challenging.

Based on these viewpoints, we developed a novel multiple solvent displacement method for the fabrication of homogeneous porous PI membranes with through-holes. This method has been applied to conduct the conventional NIPS for fabricating porous PI membranes. Generally, the NIPS method is used only for 1-stage of immersion with only one kind of solvent. The obtained dense layer on the porous PI membrane limits the applicability of the membrane only to the NF range. To overcome this limitation, multiple solvent displacements can be implemented for multi-stage immersions in different kinds of poor solvents, which can be controlled by the solvent displacement speed. As a result, the formation of a dense thin layer is decreased. Homogeneous and through-hole porous membranes can be obtained from this multiple solvent displacement method.

In this study, porous PI membranes with various pore sizes and through-holes were fabricated by the multiple solvent displacement method. In order to investigate the characteristics of the fabricated porous PI membranes, the number of immersion stages and the types of poor solvents were the main variable factors. The morphology of the surface, confirmation of the successful imidization of PI, and the efficiency of the through-hole PI membranes in air permeability were thus evaluated. This novel method is expected to be a breakthrough in porous PI membrane fabrication, which can extend the applications of PI membranes to different separation ranges.

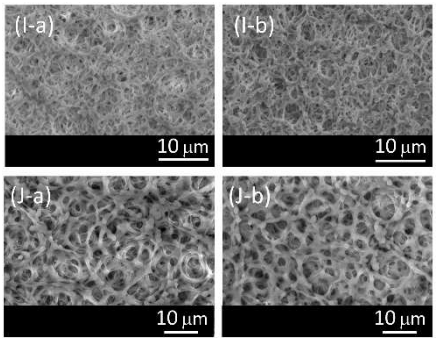


**Figure 1.** SEM images of a: PAA film, and b: PI membrane which were fabricated by 2-stage immersion (I-a, and I-b) and 3-stage immersion (J-a, and J-b).

## 2. Results and Discussion

### 2.1. Control of Pore Size by Multiple Solvent Displacement and Confirmation of Imidization

Figure 1 shows the SEM images of the PAA film (I-a for 2-stage and J-a for 3-stage) after fabrication by the multiple solvent displacement method using methanol as a poor solvent and the PI membrane (I-b for 2-stage and J-b for 3-stage) after imidization. Both, PAA and PI membranes, are detected on the highly porous surface. The structure of the PAA membrane is also nearly completely maintained in the PI membrane without any significant change due to pore clogging. In addition, there is no significant difference between 2-stage (Figure 1, I-a, and I-b) and 3-stage (Figure 1, J-a, and J-b) of solvent displacement method. This suggests that the pore structure of the porous PI membrane could be regulated when fabricating the PAA film.

Figure 2 shows the FT-IR spectra of PAA film (I-a) and PI membrane (I-b), confirming the successful imidization of the PI membrane. The aromaticity can be detected by C–H stretching near 3050 $cm^{-1}$ region, C=C stretching at 1605 $cm^{-1}$ and 1498 $cm^{-1}$, C–H out-of-plane bending at 880 $cm^{-1}$, and C–O stretching near 1200 $cm^{-1}$. These absorptions are derived from the structure of the aromatic ether in both the PAA film and PI membrane. With regard to the PI membrane (I-b), the new peaks derived from PI were significant (C=O asymmetric stretching at 1774 $cm^{-1}$, C=O symmetric stretching at 1705 $cm^{-1}$, C–N asymmetric stretching at 1362 $cm^{-1}$, and C=O bending at 737 $cm^{-1}$), whereas the characteristics of PAA disappeared from the PI membrane (O–H and N–H stretching near 2500–3500 $cm^{-1}$, C=O stretching at 1713 $cm^{-1}$, C=O stretching at 1652 $cm^{-1}$, and C–N stretching at 1532 $cm^{-1}$).[25,26] Therefore, the completion of imidization was occurred in the PI membrane as a result of calcination of the PAA film at high temperature.

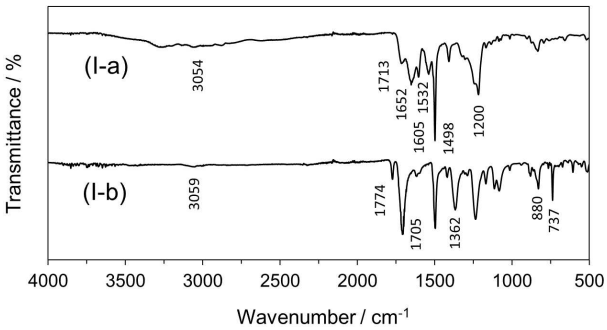


**Figure 2.** FT-IR spectra of PAA film (I-a), and PI membrane (I-b) with 2-stage immersion.

### 2.2. Surface Characterization of PI Membrane Fabricated by the Multiple Solvent Displacement Method

Figure 3 shows the SEM images of PI membranes fabricated with different number of immersion stages. For instance, the PI membrane fabricated by direct immersion only in methanol without immersion in NMP, showed porosity on the surface (Figure 3, K-series); however, the pores were localized with a non-uniform pore size on the front surface (Figure 3, K-1). These results were consistent with the theory that when PAA solution was directly immersed in a poor solvent, rapid phase separation occurs on the surface. From this reason, the aggregation of the PAA was detected which affected to the formation of a dense layer on the surface. Moreover, the dense layer was formed without any pores on the rear surface (Figure 3, K-2).

In order to decrease the solvent displacement speed, the PAA film was immersed in a mixture of NMP and methanol (as a poor solvent) prior to being immersed again in pure methanol (as a poor solvent). From the SEM images (Figure 3, L series), microscopic pores formed over the entire front surface (Figure 3, L-1); however, there was no pore formation on the rear surface (Figure 3, L-2). These results implied that it was possible to decrease the solvent displacement speed and control the rapid phase separation by multiple-stage immersion. Nevertheless, the through-hole of the PI membrane has been challenging to fabricate. Therefore, the PAA film was first immersed into an NMP solution prior to being immersed in pure methanol (as a poor solvent). Interestingly, homogenous pores were formed over the surface (Figure 3, I-1 and I-2). The 3-stages immersion was performed by immersion in NMP, the mixed solvent, and poor solvent, resulted in uniformly sized pores over the front and rear surfaces (Figure 3, J-series), which can be related to the successful fabrication of homogeneous through-holes of porous PI membrane. Thus, the multiple solvent displacement method can control the solvent displacement rate and the homogeneous through-holes can be fabricated with coinciding spinodal decomposition.

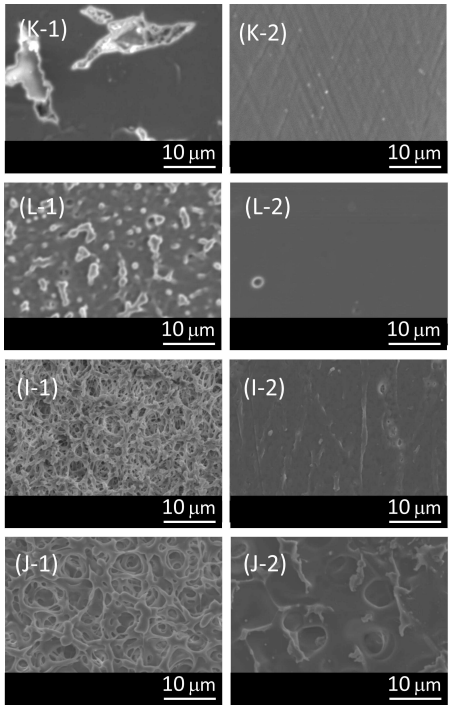


**Figure 3.** SEM images of porous PI membrane fabricated with/without immersion in NMP and different immersion stages. 1: front surface, 2: rear surface, (K) directly immersed only in methanol, (L) immersion in mixture solvent followed by direct immersion in pure methanol, (I) NMP with 2-stage immersion, and (J) NMP with 3-stage immersion.

### 2.3. Effect of Types of Poor Solvent on the Surface Morphology of the PI Membrane Fabricated from the Multiple Solvent Displacement Method

Figure 4 shows SEM images of the front surface (1), rear surface (2), and cross-section (3) of PI membranes fabricated by the multiple solvent displacement method. With the using of xylene as a poor solvent (Figure 4, A-series for 2-stage and B-series for 3-stage immersion), there is no significant difference in the morphology of PI membrane, even though the number of immersion stages are varied. Despite the fact that the PAA film was not immersed in the mixture solution, large pores were detected throughout the membrane. These can be implied to the formation of a porous structure over the entire membrane.

Similar results were detected when butyl acetate was used as a poor solvent (Figure 5, C-series and D-Series); however, the pores were smaller compared to those from xylene (Figure 4, A-series and B-series). A significant difference occurred when acetone was used as a poor solvent with different number of immersion stages (Figure 5, E-Series and F-Series). With 2-stage immersion (Figure 5, E-Series), pores were formed on the front surface, except those of a smaller with limited size that were formed on the rear surface. In contrast, with 3-stage immersion (Figure 5, F-Series), homogeneous of pores were formed over the front and rear surfaces. The porous structure of cross-section was observed and large pores were detected only in some positions on the front surface for both types of immersion stages.

The results from the using of isopropanol (Figure 6, G-Series and H-Series) and methanol (Figure 6, I-Series and J-Series) as poor solvents were similar to the one which were obtained

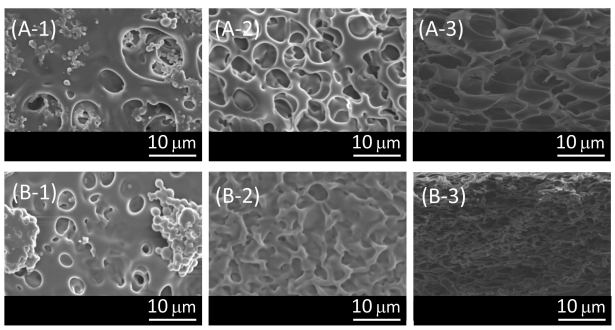


**Figure 4.** SEM images of porous PI membrane. 1: front surface, 2: rear surface, 3: cross-section; (A) xylene with 2-stage immersion, (B) xylene with 3-stage immersion.

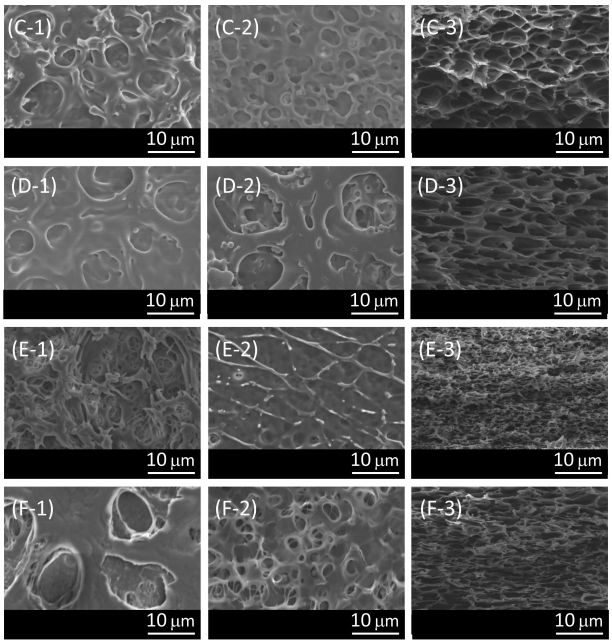


**Figure 5.** SEM images of porous PI membrane. 1: front surface, 2: rear surface, 3: cross-section; (C) butyl acetate with 2-stage immersion, (D) butyl acetate with 3-stage immersion, (E) acetone with 2-stage immersion, (F) acetone with 3-stage immersion.

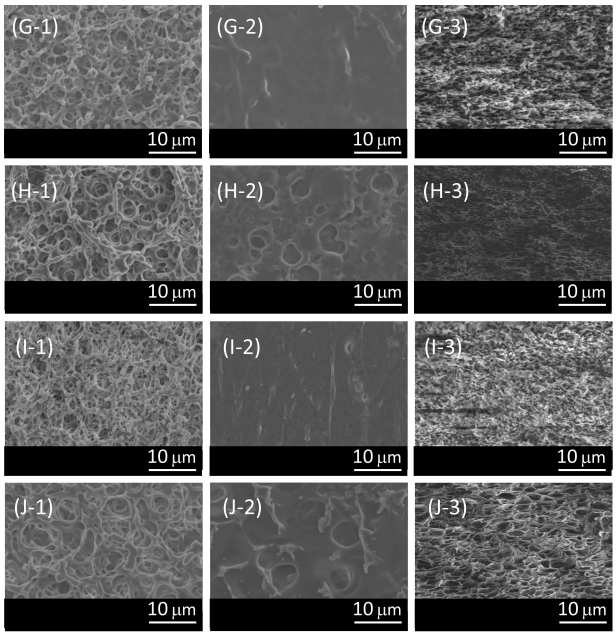


**Figure 6.** SEM images of porous PI membrane. 1: front surface, 2: rear surface, 3: cross-section; (G) isopropanol with 2-stage immersion, (H) isopropanol with 3-stage immersion, (I) methanol with 2-stage immersion, (J) methanol with 3-stage immersion.

from the using of acetone (Figure 5, E-Series and F-Series), especially in the formation of pores over the front surface. Only a few pores were observed on the rear surface after 2-stage immersion; however, the pores were detected on the rear surface after 3-stage immersion. In addition, the cross-sections of the PI membrane from the 3-stage immersion showed an obviously increase in the pore sizes compared to those formed with 2-stage immersion.

Figure 7 (M-Series and N-Series) shows the morphology of PI membrane which was used water as a poor solvent. There were no microscopic pores detected on the front surface. Moreover, no pores were formed on the rear surface even the number of immersion stages were varied. In addition, the cross-sectional images were also confirmed about the insufficient pore structure.

From these results, the using of xylene or butyl acetate as poor solvents enabled to the successful fabrication of porous PI membranes without any relationship with the number of immersion stages. Meanwhile, the 2-stage immersion was not sufficient to form the well-developed pores when acetone, isopropanol, or methanol were used as poor solvents. However, with 3-stage immersion, the PI membrane with uniform pore size and sufficient porous structure was successfully fabricated. It can be suggested that the homogeneity as well as through-holes of porous PI membrane can be controlled by selecting an appropriate poor solvent and the number of immersion stages.

### 2.4. Characterization of Porous PI Membranes: Pore Size, Porosity, Pore Volume, Thermal Properties, and Air Permeability

Table 1 summarizes the results of the pore size, porosity, air permeability, and the solubility parameter of the porous PI membranes fabricated from the multiple solvent displacement method. The solubility parameters of PAA were calculated based on the chemical structure of the substances using the Hoftyzer-Van Krevelen method and SEM images were used for the calculation of the mean pore size.[27] As the number of immersion stages increased from 2- to 3-stage, the variations in pore size between the front and rear surfaces were decreased. The 3-stage immersion was particularly important for the fabrication of a uniform porous PI membrane when using butyl acetate, isopropanol, or methanol as a poor solvent. Therefore, the multiple solvent displacement method was successfully formed uniform pores via phase separation, which enabled uniformity throughout the membrane. In addition, the pore sizes were dependent on the properties of the selected solvent.

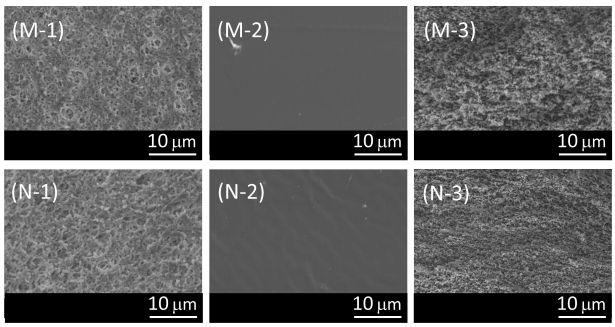


**Figure 7.** SEM images of porous PI membrane. 1: front surface, 2: rear surface, 3: cross-section; (M) water with 2-stage immersion, and (N) water with 3-stage immersion.

**Table 1.** Pore size, porosity, permeability, and solubility parameter of porous PI membranes.

| Solvent | Series | Stage | Pore Size [μm] Front | Rear | Porosity [%] | Air Permeability (Gurley value; s/100 cc)[28] | Solubility Parameter[27] $\delta$[a] | $\delta_d$ | $\delta_p$ | $\delta_h$ |
|---|---|---|---|---|---|---|---|---|---|---|
| Xylene | A | 2 | 10.1 | 7.0 | 64 | ∞[e] | 18.4[a] | 17.6 | 1.0 | 1.0 |
| | B | 3 | 12.1 | 4.5 | 66 | 4083 | 18.0[b] | 17.4 | 1.0 | 1.0 |
| | | | | | | | 18.0[c] | 17.3 | 1.0 | 1.0 |
| Butyl acetate | C | 2 | 7.3 | 4.3 | 62 | ∞ | 17.4 | 15.7 | 3.7 | 6.4 |
| | D | 3 | 9.3 | 10.0 | 64 | 1090 | | | | |
| Acetone | E | 2 | 3.0 | 2.2 | 66 | 68 | 20.5 | 15.5 | 10.4 | 7.0 |
| | F | 3 | 11.1 | 4.1 | 68 | 52 | | | | |
| Isopropanol | G | 2 | 2.1 | 1.0 | 37 | ∞ | 23.6 | 15.8 | 6.1 | 16.4 |
| | H | 3 | 2.4 | 4.9 | 53 | 2273 | | | | |
| Methanol | I | 2 | 1.7 | 1.0 | 48 | ∞ | 29.7 | 15.2 | 12.3 | 22.3 |
| | J | 3 | 3.5 | 3.6 | 66 | 553 | | | | |
| | K | 1[d] | 7.0 | 0 | 39 | ∞ | | | | |
| | L | 2[d] | 1.9 | 0 | 41 | ∞ | | | | |
| Water | M | 2 | 1.1 | 0 | 34 | ∞ | 48.1 | 14.3 | 31.3 | 34.2 |
| | N | 3 | 1.2 | 0 | 51 | ∞ | | | | |
| NMP | – | – | – | – | – | – | 22.9 | 17.9 | 12.3 | 7.2 |
| PAA | – | – | – | – | – | – | 21.9 | 19.1 | 4.3 | 9.7 |

[a] o-xylene. [b] m-xylene. [c] p-xylene. [d] Not immerse in NMP. [e] Not able to measure the air permeability

From the calculated solubility parameters in Table 1, it can be found that the smaller pores were formed with the increasing in the solubility parameters. The solvent displacement efficiency can be increased when the solubility parameter of the solvent was higher than that of NMP. Therefore, with the faster of phase separation, the smaller pores can be fabricated. Hence, the suitable selection of multiple solvents based on the solubility parameters has a significant impact on the fabrication of the porous PI membrane with the well-controlled pore size. In order to construct the homogeneous porous structure, using spinodal decomposition mechanism with effective controlling of the solvent displacement speed was necessary for preventing the development of a dense thin layer. For this reason, the multiple solvent displacement method enabled us to fabricate the porous PI membranes with thorough-holes of varying pore sizes. The different pore sizes were obtained because of the different rates of solvent displacement of PAA solution along with the suitable selection of poor solvent types.

The porosity of each porous PI membrane was calculated based on Equation (1). It can be found that PI membrane fabricated with xylene, butyl acetate, and acetone showed a high porosity of approximately 60%, without any effects from the different number of immersion stages. For those fabricated using isopropanol, methanol, and water, the smaller porosity (approximately 40%) was obtained from 2-stages immersion.

Conversely, the higher porosity (approximately 60%) was detected from 3-stage immersion. This is because the low porosity (40%) of membranes which were obtained without immersion in NMP, were not be developed by immersion in a mixed solvent. From this reason, immersion in NMP was necessary for the formation of a sufficient pore structure in a porous PI membrane.

Pore size distributions of the PI membranes were also characterized by a mercury intrusion porosimeter in order to confirm the differences in pore size and pore volume of two kinds of fabricated membranes as shown in Figure 8. It can be found that the total pore volume, median of pore diameter, and

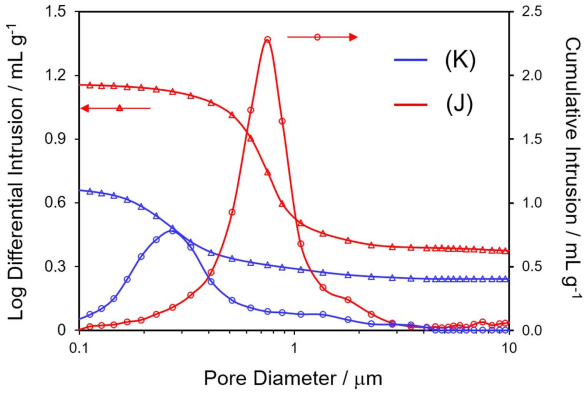


**Figure 8.** Pore size distributions of porous PI membrane. (K) direct immersion only in methanol, and (J) 3-stage immersion in NMP.

porosity of PI membrane fabricated by a direct immersion only in methanol, without an immersion in NMP (Figure 8, type (K)), were 0.69 mL/g, 0.49 μm, and 41%, respectively. In contrast, these parameters for PI membrane immersed in NMP via 3-stage immersion (Figure 8, type (J)) was 1.18 mL/g, 0.89 μm, and 53%, respectively. This result confirmed that a PI membrane fabricated with 3-stages immersion in NMP shows a significant increase in pore volume, pore diameter, and porosity which was suitable for membrane applications.

Thermal properties of the fabricated PI membrane (type K and J) were also evaluated and shown in Figure 9. Similar thermal properties were detected from two kinds of PI membranes which were fabricated from different conditions. The major thermal decomposition was occurred around 550–650 °C. The 10% of weight loss was observed at 580 °C for both types of fabricated PI membranes. Moreover, the remaining weight of fabricated PI membranes was approximately 60% at 800 °C. Table 2 summarized the comparison of thermal properties of the fabricated PI membranes from this study (type K and J) and other kinds of porous membranes. It is worth nothing that both types of fabricated PI membranes (type K and J)

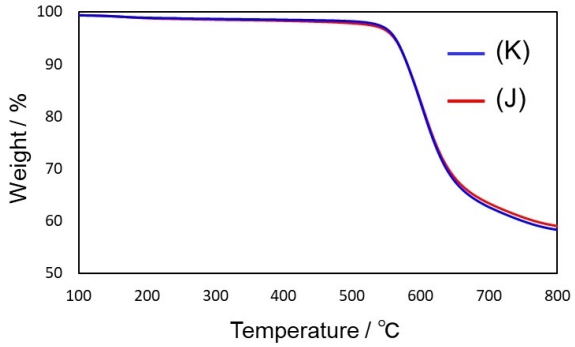


**Figure 9.** TGA curves of porous PI membrane. (K) direct immersion only in methanol, and (J) 3-stage immersion in NMP.

**Table 2.** Decomposition temperature and weight remaining of porous membranes.

| Type of Porous Membrane | Decomposition Temperature [°C] | Weight Remaining [wt%] |
|---|---|---|
| K | 550–650 | 58 (at 800 °C) |
| J | 550–650 | 59 (at 800 °C) |
| Poly(vinyl alcohol)[29] | 220–300 | 15 (at 500 °C) |
| Polyvinylidene fluoride[30] | 460–480 | 25 (at 800 °C) |
| Cellulose acetate[31] | 330–380 | 0 (at 600 °C) |

exhibit a higher decomposition temperature and the remaining weight at 800 °C than the porous membranes fabricated from poly(vinyl alcohol),[29] polyvinylidene fluoride,[30] and cellulose acetate.[31] Therefore, these fabricated PI membranes possessed high thermal properties and excellent thermal stability at high temperatures, compared to other kinds of materials which had already been used as a microfiltration (MF) or ultrafiltration (UF).

Air permeability was tested in order to confirm the efficiency of the fabricated through-hole porous PI membrane. From Table 1, the fabricated PI membranes with 2-stages immersion did not permeate air in all cases except that of acetone. On the contrary, PI membranes fabricated with 3-stages immersion showed air-permeability from the clear through-holes in all cases except water. Considering of the solubility parameter, the value of acetone is close to that of PAA. Therefore, PAA was eluted into acetone during immersion which affected to the formation of larger pore sizes on front surfaces and the formation of through-holes in relation to the high values obtained from air-permeability tests. In contrast, the solvent displacement rate was too rapid to form the through-holes in the case of water as a poor solvent, even the preparation with 3-stage immersion. PI porous membranes with microscopic pores were successfully fabricated by optimizing of the immersion time and solvent mixture conditions. From this study, the most favorable solvent for porous PI membrane fabrication was the using of methanol as a poor solvent.

## 3. Conclusion

The multiple solvent displacement method is a novel route to fabricate porous PI membranes with homogeneous pore size and through-holes. This method was facile and did not require special equipment or complicated experimental procedures. The porous PI membrane was fabricated in a simple process by only immersing the PAA film in multiple solvents prior to imidization. Owing to the pore size of the membrane be controlled by varying the types of solvent, this method has high versatility and potential for the fabrication of porous PI membranes. Further studies on the effect of mixed solvents and various immersion times on the characteristics of membrane will help to establish the applicability of this method for the fabrication of membranes with uniform and well-controlled pore sizes.

## Experimental Section

### Materials

3,4,3′,4′-Biphenyltetracarboxylic dianhydride (BPDA, >98.0% purity) was purchased from Tokyo Chemical Industry, Co., Ltd. 4,4′-Oxydianiline (ODA, >98.0% purity), the solvent N-methylpyrrolidone (NMP, >97.0% purity), xylene (>80.0%), butyl acetate (>98.0%), acetone (>99.0%), isopropanol (>98.0%), and methanol (>99.5%) were purchased from Wako Pure Chemical Industries, Ltd. All reagents were used without further purification.

### Synthesis of Polyamic Acid (PAA)

ODA (10.0 g, 50.0 mmol) and NMP (170.0 mL) were added to a nitrogen-purged separable flask and heated with stirring at 40 °C until they were completely homogeneous. Then, BPDA (14.7 g, 50.0 mmol) was gradually added into the solution every 9 hours until 3 days. Afterwards, the solution was heated while being stirred at 40 °C for 24 h, to completely consume the starting material. Subsequently, a PAA solution was obtained with a concentration of 12.4 wt% and molecular weight of 74000 g/mol.

### Fabrication of the Porous PI Membrane

Scheme 1 shows the multiple solvent displacement method used for fabricating the porous PI membrane in this study. A glass plate containing PAA solution was placed on a Tabletop Coater TC-3 (Mitsui Electric Co., Ltd., Japan). Then, a film applicator (Micron II GARDCO, Inc., USA) set to a maximum film thickness of 300 μm was used to cast PAA onto the film with a casting speed of 10 mm/s in order to control the thickness of the film (>100 μm). Afterward, the PAA film was left on a glass plate for 10 min prior to immersion in a bath containing NMP (300 mL) for 5 min and subsequently immersed in a mixture of 3:7 NMP (420 mL) and a poor solvent (980 mL). The resultant mixture was gently stirred for 15 min and finally immersed in a poor solvent (300 mL) for 15 min to form a PAA membrane by a 3-stage immersion. In the case of 2-stage immersion, the PAA film on a glass plate was immersed in NMP for 5 min prior to being immersed in a poor solvent for 15 min, dried for 24 h, and heated in a high temperature oven HTO-300S (ETTAS As One Corp., Japan), from 50 to 300 °C with a heating rate of 5 °C/min. To complete imidization, the temperature was kept stable at 300 °C for 30 min.[32] Then, the desired porous PI membrane was

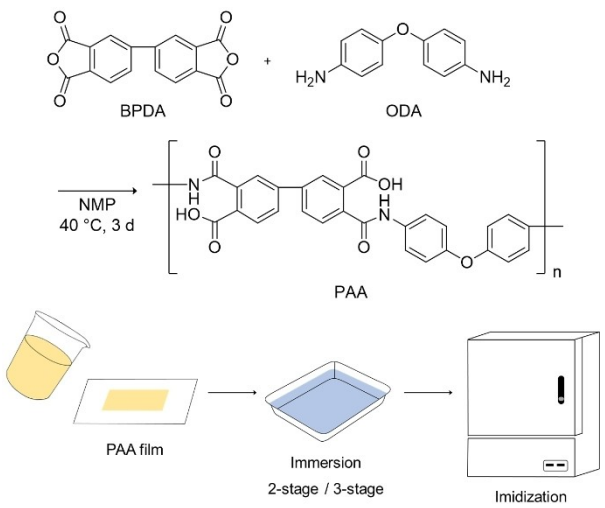


**Scheme 1.** Schematic for fabricating a porous PI membrane by the multiple solvent displacement method.

achieved soon afterwards. The variable factors in this study were the number of immersion stages (2- and 3-stage of immersion), and the kinds of poor solvent (xylene, butyl acetate, acetone, isopropanol, methanol, and water) that were summarized in Table 3.

### Characterization

In order to confirm successful imidization, Fourier-transform infrared (FT-IR) spectroscopy was conducted using a Spectrum Two (PerkinElmer Inc., Waltham, MA, USA). To confirm the morphology and pore sizes of the fabricated PI membrane, scanning electron microscopy (SEM, JSM-6060, JEOL Ltd., Japan), was employed for characterizing the front surface, rear surface, and cross-section of the membrane. The air permeability of the membrane was analyzed by a Gurley test KES–F8 Air Permeability Tester (Kato Tech Co., Ltd., Japan). The pore size and pore volume were determined using a mercury intrusion porosimeter (PoreMaster-60-GT, Anton Paar GmbH., Germany). Thermogravimetric analysis (TGA) was carried out by the SDT Q600 (TA Instruments Japan Inc., Japan) from 50 to 800 °C with a rate of 10 °C/min under nitrogen flow, while the porosity of the PI membrane was calculated as per the following equation (1):

$$porosity = 100 - \frac{m}{S \times t \times \rho} \times 100 \quad (1)$$

Here, $m$ is the mass of PI membrane (g), $S$ is the surface area of the measured PI membrane ($cm^2$), $t$ represents the membrane thickness (cm), and $\rho$ is the density of PI ($g/cm^3$). The density value used in this study was fixed at 1.39 $g/cm^3$, corresponding to the density commercial Upilex®-RN, which has the same chemical structure as PI in this study.[33] The solubility parameter consists of three factors and the equation (2) can be described as follow:

$$\delta = \sqrt{\delta_d^2 + \delta_p^2 + \delta_h^2} \quad (2)$$

Here, $\delta_d$, $\delta_p$, and $\delta_h$ represents the dispersion forces, polar forces, and hydrogen bonding interactions, respectively. According to the Hoftyzer-Van Krevelen method,[27] the solubility parameter can be predicted from the group contributions by the following equations (3)–(5):

$$\delta_d = \frac{\sum F_{di}}{V} \quad (3)$$

$$\delta_p = \frac{\sqrt{\sum F_{pi}^2}}{V} \quad (4)$$

$$\delta_h = \sqrt{\frac{\sum E_{hi}}{V}} \quad (5)$$

where $F_{di}$ represents the molar attraction constants of the dispersion [$(MJ/m^3)^{1/2}$/mol]. $F_{pi}$ represents polar components [$(MJ/m^3)^{1/2}$/mol], $E_{hi}$ represents the hydrogen bonding energy [J/mol], and $V$ represents the molar volume ($cm^3$/mol).

**Table 3.** The number of immersion stages and the kinds of solvents used for the fabrication of the porous PI membrane

| Series | Number of stages | First Immersion | Second Immersion | Third Immersion |
|---|---|---|---|---|
| A | 2 | NMP | Xylene | – |
| B | 3 | NMP | NMP/Xylene | Xylene |
| C | 2 | NMP | Butyl acetate | – |
| D | 3 | NMP | NMP/Butyl acetate | Butyl acetate |
| E | 2 | NMP | Acetone | – |
| F | 3 | NMP | NMP/Acetone | Acetone |
| G | 2 | NMP | Isopropanol | – |
| H | 3 | NMP | NMP/ Isopropanol | Isopropanol |
| I | 2 | NMP | Methanol | – |
| J | 3 | NMP | NMP/Methanol | Methanol |
| K | 1 | Methanol | – | – |
| L | 2 | NMP/Methanol | Methanol | – |
| M | 2 | NMP | Water | – |
| N | 3 | NMP | NMP/Water | Water |

## Conflict of Interest

The authors declare no conflict of interest.

**Keywords:** porous polyimide membranes · pore size control · nonsolvent induced phase separation · multiple solvent displacement method · through-hole

[1] E. P. Favvas, F. K. Katsaros, S. K. Papageorgiou, A. A. Sapalidis, A. C. Mitropoulos, *React. Funct. Polym.* **2017**, *120*, 104–130.
[2] H. Wang, T. Wang, S. Yang, L. Fan, *Polymer* **2013**, *54*, 6339–6348.
[3] A. Moslehyani, M. Mobaraki, A. F. Ismail, T. Matsuura, S. A. Hashemifard, M. H. D. Othman, A. Mayahi, M. R. DashtArzhandi, M. Soheilmoghaddam, E. Shamsaei, *React. Funct. Polym.* **2015**, *95*, 80–87.
[4] S. Leong, A. Razmjou, K. Wang, K. Hapgood, X. Zhang, H. Wang, *J. Membr. Sci.* **2014**, *472*, 167–184.
[5] B. van der Bruggen, C. Vandecasteele, T. van Gestel, W. Doyen, R. Leysen, *Environ. Prog.* **2003**, *22*, 46–56.
[6] M. Razali, J. F. Kim, M. Attfield, P. M. Budd, E. Drioli, Y. M. Lee, G. Szekely, *Green Chem.* **2015**, *17*, 4034–4059.
[7] A. Figoli, T. Marino, S. Simone, E. D. Nicolò, X.-M. Li, T. He, S. Tornaghi, E. Driolia, *Green Chem.* **2014**, *16*, 5196–5205.
[8] K. Han, W. Xu, A. Ruiz, P. Ruchhoeft, S. Chellam, *J. Membr. Sci.* **2005**, *249*, 193–206.

[9] Y. Yamauchi, N. Suzuki, T. Kimura, *Chem. Commun.* **2009**, *38*, 5689–5691.
[10] M. Ulbricht, *Polymer* **2006**, *47*, 2217–2262.
[11] F. Fan, L. Wang, H. Liu, *Mater. Lett.* **2017**, *198*, 124–127.
[12] R. Roche, F. Yalcinkaya, *ChemistryOpen* **2019**, *8*, 97–103.
[13] A. Tiwari, E. Sancaktar, *Eur. Polym. J.* **2018**, *103*, 220–227.
[14] Z. Hu, Y. Lu, X. Zhang, X. Yan, N. Li, S. Chen, *Front. Mater.* **2018**, *12*, 156–167.
[15] J. F. Kim, J. H. Kim, Y. M. Lee, E. Drioli, *AIChE J.* **2016**, *62*, 461–490.
[16] Z. Cui, Y. Cheng, K. Xu, J. Yue, Y. Zhou, X. Li, Q. Wang, S.-P. Sun, Y. Wang, X. Wang, Z. Wang, *Polymer* **2018**, *141*, 46–53.
[17] Z. Li, H. Zou, P. Liu, *RSC Adv.* **2015**, *5*, 37837–37842.
[18] G. R. Guillen, Y. Pan, M. Li, E. M. V. Hoek, *Ind. Eng. Chem. Res.* **2011**, *50*, 3798–3817.
[19] M. Chen, W. Zhou, J. Zhang, Q. Chen, *Polymer* **2020**, *12*, 322.
[20] D.-J. Liaw, K.-L. Wang, Y.-C. Huanga, K.-R. Lee, J.-Y. Lai, C.-S. Ha, *Prog. Polym. Sci.* **2012**, *37*, 907–974.
[21] Y. Li, B. Cao, P. Li, *Appl. Surf. Sci.* **2019**, *473*, 1038–1048.
[22] M. Z. Ahmad, H. Pelletier, V. Martin-Gil, R. Castro-Muñoz, V. Fila, *Membranes* **2018**, *8*, 67.
[23] Y. Chen, L. Ying, W. Yu, E. T. Kang, K. G. Neoh, *Macromolecules* **2003**, *36*, 9451–9457.
[24] M. Kim, G. Kim, J. Kim, D. Lee, S. Lee, J. Kwon, H. Han, *Microporous Mesoporous Mater.* **2017**, *242*, 166–172.
[25] E. Han, Y. Wang, X. Chen, G. Shang, W. Yu, H. Niu, S. Qi, D. Wu, R. Jin, *ACS Appl. Mater. Interfaces* **2013**, *5*, 4293–4301.
[26] K. P. Pramoda, S. Liu, T.-S. Chung, *Macromol. Mater. Eng.* **2002**, *287*, 931–937.
[27] D. W. van Krevelen, K. te Nijienhuis, Properties of polymers: Their correlation with chemical structure; their numerical estimation and prediction from additive group contributions, fourth Ed., Elsevier Science, Amsterdam, the Netherlands, **2009**.
[28] K. Prasanna, C. W. Lee, *J. Solid State Electrochem.* **2013**, *17*, 1377–1382.
[29] Y. Yuan, J. Liu, C. Li, J. Fang, S. Wang, R. Guan, *J. Appl. Polym. Sci.* **2011**, *122*, 3071–3079.
[30] D. Cheng, L. Zhao, N. Li, S. J. D. Smith, D. Wu, J. Zhang, D. Ng, C. Wu, M. R. Martinez, M. P. Batten, Z. Xi, *J. Membr. Sci.* **2019**, *588*, 11724.
[31] H. Sanaeepur, A. Kargari, B. Nasernejad, *RSC Adv.* **2014**, *4*, 63966–63976.
[32] H. Inoue, Y. Sasaki, T. Ogawa, *J. Appl. Polym. Sci.* **1996**, *60*, 123–131.
[33] UBE Industries, Ltd., Ultra heat-resistant film. http://www.upilex.jp/en/upilex_grade.html#02 (accessed Sep 10, 2020).

Manuscript received: October 6, 2020
Revised manuscript received: January 19, 2021